

# Cover Requirement and Stability of Horizontally Bent Buried Pipelines

Hamdan N. Al-Ghamedy, e-mail: [hghamdi@kfupm.edu.sa](mailto:hghamdi@kfupm.edu.sa), fax: +966 3 860 2694  
Sahel N. Abduljawwad, Junaid A. Siddiqui,  
Naser A. Al-Shayea, and Ibrahim M. Asi

Department of Civil Engineering  
King Fahd University of Petroleum & Minerals  
Dhahran 31261, Saudi Arabia

**Abstract.** *The soil cover requirement for horizontally bent buried pipeline is discussed. The variables considered in this research include the pipe diameter and thickness, the radius and angle of the bend, the internal pressure, the fluid specific weight, the overburden height, the temperature rise, and the material used. A comprehensive three-dimensional finite element analysis is run. The results obtained are utilized to develop regression models for the maximum allowed temperature change as well as the minimum overburden height. The relationships among the different variables are determined. To guard against elastic instability, several buckling mode are checked.*

## Introduction

Cross-country pipelines are very common worldwide. Although some are utility pipes, such as water, many of them are used in the oil industry to transport gas and other petroleum products. These pipelines are often buried underground. Due to reasons related to the terrain, economy, and right of way, it is sometimes necessary to bend the pipe; this paper is concerned with horizontal-type bends. Compared with straight ones, the behavior of bent pipes is quite different and more complicated; this is particularly true under temperature rise. In order to fully and deeply study this problem, many variables need to be accounted for. These variables include the pipe diameter, pipe thickness (or  $D/t$  ratio),

bend radius, bend angle, internal pressure, fluid specific weight, overburden (soil) height, temperature change, pipe material, and soil type.

Although there exists some work carried out in the past related to buried pipes, as discussed below, no comprehensive study has been done on horizontally bent pipelines with the variables stated above. Some codes/standards have special provisions for bends. For example, the code of the American Society of Mechanical Engineers ASME B31.4 [1] uses a flexibility factor and a stress intensification factor, utilizing simple beam theory, to account for the flexural behavior of the pipe bent. Saudi Arabian Oil Company (Saudi Aramco), which is the biggest oil company in the world, uses a simplified theory in its standard SAES-L-051 [2] for estimating the soil cover requirement for buried bent pipes. The first theoretical work for smooth unrestrained bends was done by Karman [3]; other studies followed, e.g. Vigness [4], Pardue and Vigness [5], Kafka and Dunn [6], Rodabaugh and George [7], Findlay and Spence [8]. In the last two decades, some studies were carried out. Thomson and Spence [9] presented new analytical solutions. Whatham [10] utilized thin shell theory. An analytical model for the elastic/plastic design of pipe bends was formulated by Gresnigt and van Foeken [11].

Utilizing the finite element method (FEM), different design aids were developed by Natarajan and Blomfield [12], Ohtsubo and Watanabe [13], and Weiß et al. [14]. To model the pipe bend, either beam-shell or shell-ring element was used. Hibbett [15], Bathe and Almeida [16], and Mackenzie and Boyle [17] utilized the first type, while Ohtsubo and Watanabe [13] and De Melo and De Castro [18] used the second one (shell-ring/pipe element). Yin et al. [19], Altaee and Boivin [20], and Altaee et al. [21] did some analyses for different soils.

The soil resistance against movement was first studied by Winkler [22], who introduced the concept of subgrade reaction, followed by Hetenyi [23]. Afterwards, Vesić

[24], Audibert and Nyman [25], Peng [26], Nyman [27], Hsu [28], Goodling [29], and Ng et al. [30] conducted more studies.

An extensive laboratory study of the uplift and lateral movement of buried pipes was carried by Trautmann et al. [31,32], and the results were compared with that of Ovesen [33], Vesić [24], Audibert and Nyman [25], and Row and Davis [34]. Hsu [35] studied the velocity effects, while Dickin [36] and Poorooshab et al. [37] carried out some centrifuge model studies.

### **Horizontal Bend Problem and Research Program**

Buried pipelines could experience significant longitudinal deformations due mainly to temperature rise (because of the hot fluid) and internal pressure; as a result, instability problem could arise if there is a bend. The earth pressure of the confining soil helps in resisting the movement; therefore, the strength of the soil is quite important to keep the buried pipe bend adequately restrained against excessive deformation. Even though they have proven to be inadequate in modeling the actual field behavior of pipe-soil systems, classical theories-based methods have been and are still being used. Lately, some numerical methods are utilized as summarized above but due to the effort required in modeling the complex pipe-soil composite system, their application is limited. In the current research, a very comprehensive investigation on the soil cover requirement and stability of horizontally bent pipelines is carried out utilizing three-dimensional finite element modeling. This problem of horizontally bent pipelines is commonly encountered in field, especially in the oil industry. The parameters considered in this study include the pipe diameter, pipe thickness, bend radius, bend angle, internal pressure, fluid specific weight, temperature change, overburden height, pipe material, and soil type. With all these

variables accounted for, a general method for the analysis and design of buried horizontal bends is developed.

Several steps are followed to execute the research program and achieve the objectives. First, a literature survey on the subject is done. Second, an appropriate software package, which serves our needs, is chosen. Next, a three-dimensional FEM model, which is capable of simulating the soil-horizontal pipe bend system, is set and validated. After that, a complete and comprehensive analysis, taking into account the combinations and interactions among all the variables stated above, is carried out. Finally, utilizing the results from the previous step, regression models, which can be used for the analysis and design, are developed.

### **Material Models**

The material of the pipe used in the study is steel. Any grade can be used; however, the behavior was assumed to remain within the linear elastic range, as the working stress is usually restricted to be below the yield strength with an appropriate safety factor. Soil, on the other hand, is neither linear nor elastic. Sand, which is the most common type in the local environment, was used in the investigation; therefore, and among other tried theories, Mohr-Coulomb material model was assumed as the failure criterion. For the material parameters needed in this research, the steel properties are specified by the manufacturer and/or standard(s), while for loose/uncompacted sand, which is always used as the trench backfill material, the necessary experiments, e.g. triaxial and direct shear tests, were carried out to determine all needed strength parameters; the angle of internal friction ( $\phi$ ) =  $35^\circ$ , and the cohesion ( $c$ ) = 0. For the “artificial” (fictitious) interface/joint elements, the properties assumed are discussed in the numerical analysis section of the paper.

## Preliminary Validation Runs

Before carrying out the full numerical analysis and the parametric study, some preliminary considerations are warranted. First, the software to be used for the analysis was selected. Among many options and taking many factors into considerations, the program Structure Medium Analysis Program (SMAP-3D) [38] was chosen. This FEM-based package met our needs when the features it has were inspected. For the pre and postprocessing, the program Finite Element Modeling And Postprocessing (FEMAP) [39,40] was utilized, as will be discussed in a later section of the paper.

With the absence of previous experimental and/or analytical work in the same or similar area, it became quite necessary to test and validate the models and procedures used in this study. In order to study and compare individual structural response and phenomena, several numerical tests were run. The arching effect of the soil, the discretization, mesh refinement and element size effect, and the soil resistance to the lateral movement of a straight pipe were all examined.

The arching effect of very flexible and rigid pipes was checked. Several runs were executed. The elastic moduli assumed were 200 GPa (29000 ksi) and 690 MPa (100 ksi), the thicknesses were 152 mm (6 in.) and 6.35 mm (0.25 in.) for the rigid and flexible pipes, respectively, while the diameter selected was 1219 mm (48 in.) for both. Cover depths of 762 mm (30 in.), 1067 mm (42 in.), 1524 mm (60 in.), and 2286 mm (90 in.) were used. Deformations as well as stresses were obtained. The results were compared with the formulas of Marston and Anderson [41] and found to be similar in the *overall* behavior and trend. However, the equations were based on certain assumptions and approximation leading to the belief that as far as *numbers* are considered, the FEM solution is more accurate. Details can be found in ref. [42].

Since the 3-D soil-horizontally bent pipe system is quite involved, as far as the FEM is concerned, it is important to generate a mesh which is reliable as well as optimum/efficient and which can run in the computer and with the software at hand. As a result, many meshes, with different discretizations and element sizes, were used in trial/test runs. For example, four different two-dimensional meshes, which were used to generate the three-dimensional meshes as will be discussed later in the paper, are shown in Fig. 1; they range from a very fine mesh with all square elements to a relatively coarse mesh with slender elements. When a horizontal line force (force per length) is applied on the center (springline) of the pipe, the pipe tries to move horizontally in the same direction. Such results obtained for the meshes with different densities are plotted in Fig. 2. As can be seen, all results are close to each other, concluding that no need to have a “too refined” mesh with square elements; the relatively coarse meshes are “good enough”.

To further validate the model for the horizontal movement of buried pipes (before starting the full bend analysis), the well documented and cited experiments carried out by Trautmann and O'Rourke [32] [also appeared in other previous publications] were simulated by a 3-D FEM mesh, and the two results were compared. The use of the findings of their full-scale laboratory tests has been recommended in different publications such as ASME B31.1 [43] and CGL [44]. The pipe diameter was 101.6 mm (4 in.), the thickness was 6.35 mm (0.25 in.), cover depths of 152.4 mm (6 in.) 355.6 mm (14 in.), 812.8 mm (32 in.), and 1117.6 mm (44 in.) were tried while loose [ $\gamma = 14.8 \text{ kN/m}^3$  (94.2 pcf),  $\phi = 31^\circ$ ], medium [ $\gamma = 16.4 \text{ kN/m}^3$  (104.4 pcf),  $\phi = 36^\circ$ ], and dense [ $\gamma = 17.7 \text{ kN/m}^3$  (112.7 pcf),  $\phi = 44^\circ$ ] sands were used.

The maximum force obtained in the analysis was chosen to be the point in the load-deformation plot beyond which the curve became relatively flat. The strength of the soil against the lateral movement of the buried pipe, quantified by a dimensionless factor  $N_h$ ,

for each run is shown in Fig. 3 along with the experimental data of Trautmann and O'Rourke [32]. It can be noticed that good agreement is obtained in some of the points, while some discrepancies are present in others. In particular, the over prediction for larger cover depths could be attributed to the fact that analytical models do not account for the large volume reductions which occur during shear. For the dense sand, one of the possible reasons for the difference could be related to the value used for  $\phi$ . In the experiment, a direct shear test was used to determine it, while in the 3-D FEM analysis it is more appropriate to use the value from a triaxial test, which was not reported in the lab tests; the difference between the two values could range from 1 to 5 degrees. In addition, as stated by Trautmann and O'Rourke, there could be some uncertainty/variation in the measurement of  $\phi$  (between different researchers); moreover, the "exact" determination of the maximum force in some cases was not possible. It is also worth mentioning that, as stated in the original paper, in some previous work the force was overpredicted by as high as 200%. We may add that in the field (especially in oil industry), the depth (or  $H/D$  ratio) rarely, if ever, gets as high as the values used in the experiments for the deep pipes, which gave the largest error/difference. Reference [45] shows more details and it can be reviewed.

### **Finite Element Modeling and Analysis**

The next step, which is the major one, in this study is the finite element modeling of the 3D system and the analysis which follows. The procedures are summarized below.

**Virtual Anchor and Influence Length.** The so-called virtual anchor and influence length of the pipe are needed to be introduced first. Cross-country buried pipelines could run for hundreds of miles (kilometers), which can be considered mathematically as infinitely long. Thus, when a bend is to be analyzed or designed, a "virtual anchor" needs

to be assumed or specified in order to “truncate” the pipe/soil system. A typical model for buried horizontal pipe bend is drawn in Fig. 4. The lateral movement of a horizontal pipe bend is resisted by the passive soil pressure  $\sigma_h$ , as shown in Fig. 4, and the shear strength of the soil  $\tau_s$ . When a buried pipe is moved horizontally, the soil displacement field around the pipe causes it to move in an upward direction as well, as illustrated in Fig. 5. Thus, in addition to the resistance given by the soil, the movement of the pipe is also counteracted by the weight of the pipe and its contents. When a straight pipe connected to a bend expands due to a temperature increase and/or internal pressure, it causes the bend apex to move. In addition to the bend, a length of the straight pipe also moves transversely relative to the soil and it is called *influence length*  $L_{inf}$ , as shown in Fig. 4. The lateral movement along the influence length is caused by the in-plane bending moment transferred by the bend to the straight pipe. It is given by:

$$L_{inf} = \frac{3\pi}{4\beta} \quad (1)$$

which is the length at which the hyperbolic function given by Hetenyi [23] approaches unity;  $\beta$  is a parameter which represents the pipe-soil system characteristics that depends on the modulus of subgrade reaction,  $k$ , and the pipe stiffness,  $EI$  (elastic modulus and moment of inertia). Thus, according to ASME B31.1 [43]:

$$\beta = \sqrt[4]{\frac{k}{4EI}} \quad (2)$$

The friction between the pipe and the soil restrains the longitudinal movement of the straight pipe relative to the soil. The maximum movement occurs at the end of the pipe where the bend is connected and starts to be reduced from there to a point beyond which there is no movement of the pipe relative to the soil. It is that point which is called *virtual anchor*. The location of the virtual anchor,  $L_{va}$ , is required for the geometry and to provide the appropriate boundary conditions for the three dimensional mesh. ASME B31.1 [43] recommends the following formula:

$$L_{va} = \Omega \left[ \sqrt{1 + \frac{2 F_{\max}}{f \Omega}} - 1 \right] \quad (3)$$

where  $\Omega$  is an effective length parameter given by:

$$\Omega = \frac{A E \beta}{k} \quad (4)$$

$F_{\max}$  is the maximum axial force in the pipe;

$f$  is the unit soil friction force along the pipe;

$A$  is the cross-sectional area of the pipe.

**FEM Modeling and Mesh Generation.** As a semi-infinite domain extending infinitely in the horizontal direction and downward, the soil system needs to be truncated at a place where the geo-static condition exists. The limits used to truncate the FEM mesh and specify the free field condition are illustrated in Fig. 6. These limits were concluded based on the observation made during the trial/test runs, using the SMAP and CANDE [46] programs, as well as the recommendations stated in the literature (e.g. Altaee et al. [21] and Row and Davis [34]). Each of the width behind and below the pipe was taken as the larger of that required by the gravity loading and that required for the pipe horizontal movement.

The development and generation of the three dimensional mesh of the soil-pipe bend system was achieved using the program FEMAP. The strategy used in that program was, first, the generations of a two dimensional mesh along the pipe cross-section; then the two dimensional mesh was extruded along the pipeline longitudinal axis to obtain the desired three dimensional mesh. For the soil, continuum elements characterized by Mohr-Coulomb failure theory were used, while for the pipe shell elements were utilized. For the pipe-soil interface, joint elements were assumed to exist. Since the joint element occupies a region which does not physically exist, it is therefore desirable to keep the thickness of the element as small as possible; however, during the validation runs it was found that convergence could not be achieved when a very small value for the thickness was used. Therefore, the smallest possible value was used; it came out to be  $D/40$  where  $D$  is the pipe diameter. In addition, the numerical analysis came out to be sensitive to the value of the shear parameter,  $G$ , used for the interface element; this is due to the longitudinal movement of the pipe relative to the soil. After many trial numerical tests, a value of 172 kPa (25 psi) came out to be appropriate as long as the cover depth was not less than 305 mm (12 in.). For shallower pipes, a smaller value for  $G$  needed to be used.

Figure 7 shows a typical two dimensional mesh which was used to generate the three dimensional mesh. For the pipe ring, 24 linear shell elements were used. As stated above, continuum elements characterized by Mohr-Coulomb model were utilized for the soil except a layer of elements just behind the pipe; it was assigned a linear elastic model. This was required because as the pipe moved laterally, a void was generated behind the pipe, which caused solution instability if Mohr-Coulomb criterion was used for these elements behind the pipe. As the 3D mesh size could get very large, especially if there is a lack of (some) symmetry, a compromise between the element size/aspect ratio and the accuracy needed was made (using and taking advantage of the conclusions and observations made

during the preliminary runs discussed before). However, it can be seen from Fig. 7 that a very fine mesh and square, or almost square, elements were kept in the critical regions, e.g. segments 1 to 3. The next step was the extrusion of the 2D mesh to a 3D mesh. Due to the nature of the problem and the boundary conditions, this procedure is quite lengthy and relatively complex in geometry, so detail is not presented here since it is mainly geometric manipulations [47]. However, a typical generated 3D mesh is shown in Fig. 8 in which the one plane of symmetry was taken advantage of such that half of the domain only is shown with appropriate boundary conditions.

### **Loads on Pipe**

The loads which act on the pipe include the soil above it, the pipe weight and its contents, the internal pressure, and the temperature. Since the problem is nonlinear, the loads were applied in increments and within each increment iterations were performed until the solution converges. From the experience gained from the previous runs, and after many trial tests, the loading was divided to 20 steps. If there was any numerical instability or divergence, then appropriate parameters were tuned and a rerun was carried out until convergence was achieved.

### **Parameteric Study**

From the preliminary work and setup discussed above, confidence was gained such that a general and comprehensive parametric study was prepared and made ready to be executed. Utilizing the FEM, an extensive and lengthy numerical analysis program was carried out; the results of interest were extracted from the large volume of output obtained. Full details of the runs are not presented here, but rather sample results and key issues are included in the paper.

The variables/parameters studied in this research are the pipe diameter, overburden height, bend radius, bend angle, pipe thickness (diameter/thickness ratio), internal pressure, fluid specific gravity, temperature change, allowable stress, safety factor, modulus of soil reaction, and Winkler spring coefficient. The ranges (minimum-maximum values) for these parameters are listed in Table 1. In the FEM runs, carefully selected values were used within the ranges; more emphasis was placed on critical values/limits and intermediate points in order to develop reliable and general models as will be discussed later in the paper. Many different combinations of the variables were considered in the analysis so that the effect of each individual parameter as well as the interaction among them were all taken into account.

Before elaborating more on the results, it is first important to define the capacity of buried pipe horizontal bends due to the applied loads which include temperature change, gravity loads, and internal pressure. There are two different ways to define such a capacity. The first one, which is economical and named by the authors as the ultimate temperature/load method defines the point when the soil reaches its passive strength due to the pipe horizontal/vertical movement. This implies that the pipe will move a distance before the shear failure, which means that the soil would “flow” under the pipe. This may lead to a continuing process with time until the pipe is exposed. Such an action is not allowed by some oil companies like Saudi Aramco; thus, it is not considered here even though some results were obtained. The second way or method for calculating the capacity is termed by the authors as the installation condition method. In this method, the upward movement of the bend under the action of the total loading is restricted to the installation condition, which is defined as the state of the trench before the pipe is placed. After the installation of the pipe is complete, there will be initial/permanent settlement due to the weight of the soil cover and pipe. According to this method, the allowed upward

movement of the bend apex due to the temperature rise and internal pressure is equal to that initial settlement. In calculating the total initial settlement by the FEM, it is necessary to subtract the contribution from the mesh *below* the pipe under its own weight (before placing the pipe and filling the trench) from the total settlement. More details can be found in ref. [47].

A complete list of the results from the analysis was obtained; however, due to its large volume, a summary sample is presented in Table 2. These results, which were extracted from the whole output, are a partial list of the results of interest that were used to develop general models as will be explained below. The 3D FEM analysis took several months to run on the latest Pentium process. Most of the time, each single run took several hours to complete, while some took few days, even though every effort was made to optimize as well as minimize the runs (without affecting the results). For the full results, ref. [48] can be consulted.

### **Regression Analysis**

The database generated from the FEM analysis was utilized to develop regression models for the horizontally bent pipelines. The dependent variable could be set as the ultimate temperature change,  $\Delta T$ , or the required cover height,  $H$ . The design variables used in developing the regression equations are the depth of cover, or the ultimate temperature change, pipe diameter, diameter/thickness ratio, radius of bend, angle of bend, internal pressure, and specific gravity of the transported fluid.

A correlation matrix was obtained in order to check the relationships among the different variables used in the development of the regression models. Upon examining such a matrix, it was found out that the resulted models could be improved if the data was grouped according to the behavior. Therefore, after studying deeply different possibilities,

it was found best if these groups were formed based on the bent angles. The first group was for small pipe bends (from 1° to 15°), the second group was for intermediate pipe bends (from 15° to 45°), and the third group was for large bends (from 45° to 90°). Thus, separate models were generated for each group of data.

The regression analysis was performed utilizing the program package STATISTICA 6.1. Table 3 presents the resulting regression equations for the three groups of data. The original database used and the analysis carried out were in U.S. customary units as shown in the table; thus, the coefficients and the variables in the models must be in such units. The conversion factors from these units to the SI units are written at the bottom of the table; however, such conversion factors are programmed in the computer so that the user can select the SI units, and the program automatically converts the SI units into the appropriate units at the beginning of the analysis and at the end to show the results in the standard SI units. The SI units user does not “feel” it. The authors thought that this is the easiest/best way of doing it for two main reasons. First, it is not worth changing all the units in the database, regression analysis, etc. since the program accepts either of the two systems of units and make the appropriate conversion without the user’s interference. Second, some societies/associations/individuals still use the U.S. Customary units, or at least they allow their usage. It can be noticed in Table 3 that all coefficients of determination,  $R^2$ , are higher than 0.880. In addition, all confidence levels are higher than 99.99%.

Since in oil industry *either* the minimum required cover height,  $H$ , or the maximum allowable temperature change,  $\Delta T$ , is needed, then two forms of the regression equations are written. One is used to determine  $\Delta T$  as a function of the other variables; this form is appropriate for checking *existing* situations/design. The second form is utilized to calculate  $H$  as a function of the remaining variables; it is suitable for the actual (initial)

design of the bent buried pipelines at hand. For data values falling between two different groups, the computer program makes the necessary and appropriate interpolations.

### **Buckling of Buried Pipelines**

Large pipes with small thickness are liable to different types of buckling. In some cases, a buried pipe could buckle before it tries to bow up; therefore, it is important to check buckling along with the analysis/check discussed above. The subject of shell-type structure's buckling could get complicated; the buckling of "flexible" buried pipes is even more complex. A comprehensive survey of the literature on the subject is carried and is summarized below. No "exact" theories and/or full experimental work exist for all possible modes of buckling for such a structural system. Thus, whatever appropriate work carried in the past, which could be applicable in this study, was utilized in the current research. Of course, this implies that the assumptions/limitations of those works must also be carried to this study; the references cited can be consulted for full explanations and details. The buckling modes accounted for in these investigations are listed below.

- (1) *Buckling of cylindrical shells under the action of uniform axial compression:* axial buckling by warping [49–52].
- (2) *Buckling of cylindrical shells under the action of uniform external pressure:* ring buckling [49,50,53–56].
- (3) *Pure bending buckling:* wrinkling due to longitudinal bending [50,53, 57–65].
- (4) *Lateral beam and shell buckling:* Beam-column/shell [50,66–71].
- (5) *Buckling due to the combined effect of the stress components:* [53,72,73].

A buckling mode for *initially-bent* pipes was not considered here; this is because the pipe has to buckle vertically while the initial bend ( $\delta$ ) is in the horizontal direction. Thus, this “initial imperfection” was ignored.

The above buckling modes were checked utilizing the results of the FEM analysis. If there was any kind of buckling, then the problem had to be reanalyzed/redesigned again after making the necessary modifications (e.g. increase the pipe thickness). More details can be found in ref. [74].

### **Computer Software**

After completing a lengthy and comprehensive research program on buried pipelines, from which the results presented in this paper was extracted, a software package, named by the authors Analysis and Design of Buried Pipelines (ADBP), was developed for personal computers [75]. It is users’ friendly and quite general on that particular subject. All desired analysis, design, and checks are carried out in it; it is well-tested, robust, and can easily be expanded.

### **Summary and Conclusions**

A comprehensive three dimensional finite element analysis of horizontally bent buried pipelines was carried out to study the soil cover requirement and stability due to loading. The loads include gravity, internal pressure, and temperature variations. The factors of importance include the pipe diameter and thickness, the radius and angle of bend, the material used, the soil cover height, the temperature change, the fluid specific weight, and the internal pressure. Good regression equations were derived from the results obtained; they calculate the maximum allowable temperature rise and the minimum overburden

cover requirement. The entire research results were incorporated into a computer program. The resulted software is capable of making all necessary analysis, design, and checks.

### **Acknowledgements**

The support and cooperation of the Consulting Services Department in Saudi Arabian Oil Company (Saudi Aramco) is very much appreciated. The support of King Fahd University of Petroleum & Minerals in general and the Civil Engineering Department and the Research Institute in particular is also acknowledged.

### **References**

- [1] ASME B31.4, 1992, *Liquid Transportation Systems for Hydrocarbons, Liquid Petroleum Gas, Anhydrous Ammonia, and Alcohols*, ASME, New York.
- [2] SAES-L-051, 1998, "Construction Requirements for Cross-Country Pipelines," *Saudi ARAMCO Engineering Standard*, Saudi Arabian Oil Company (Saudi ARAMCO), Saudi Arabia.
- [3] Karman, Th. von, 1911, "Über die Formänderung dünnwandiger Rohre, insbesondere federnder Ausgleichrohre," *Zeitschrift des Vereines deutscher Ingenieure*, **55**(45), pp. 1889–1895.
- [4] Vigness, I., 1943, "Elastic Properties of Curved Tubes," *Trans. ASME*, pp. 105–120.
- [5] Pardue, T. E., and Vigness, I., 1951, "Properties of Thin Walled Curved Tubes of Short Bend Radius," *Trans. ASME*, **73**, pp. 77–84.
- [6] Kafka, P. G., and Dunn, M. B., 1956, "Stiffness of Curved Circular Tubes With Internal Pressure," *Trans. ASME*, **78**, pp. 247–254.

- [7] Rodabaugh, E. C., and George, H. H., 1957, "Effect of Internal Pressure on Flexibility and Stress Intensification Factors of Curved Pipe or Welding Elbow," *Trans. ASME*, **79**, pp. 939–948.
- [8] Findlay, G. E., and Spence, J., 1979, "Stress Analysis of Smooth Curved Tubes With Flanged End Constraints," *Int. J. Pressure Vessels and Piping*, **7**, pp. 83–103.
- [9] Thomson, G., and Spence, J., 1983, "Maximum Stresses and Flexibility Factors of Smooth Pipe Bends With Tangent Pipe Terminations Under In-Plane Bending," *ASME J. Pressure Vessel Technol.*, **105**, pp. 329–336.
- [10] Whatham, J. F., 1986, "Pipe Bend Analysis by Thin Shell Theory," *ASME J. Appl. Mech.*, **53**, pp. 173–180.
- [11] Gresnigt, A. M., and van Foeken, R. J., 1995, "Strength and Deformation Capacity of Bends in Pipelines," *Int. J. Offshore Polar Eng.*, **5**(4), pp. 294–307.
- [12] Natarajan, R., and Blomfield, J. A., 1975, "Stress Analysis of Curved Pipes With End Constraints," *Comput. Struct.*, **5**, pp. 187–196.
- [13] Ohtsubo, M., and Watanabe, O., 1977, "Flexibility and Stress Factors of Pipe Bends—An Analysis by the Finite Ring Method," *ASME J. Pressure Vessel Technol.*, **99**, pp. 281–290.
- [14] Weiß, E., Lietzmann, A., and Rudolph, J., 1996, "Linear and Nonlinear Finite-Element Analyses of Pipe Bends," *Int. J. Pressure Vessels Piping*, **67**(2), pp. 211–217.
- [15] Hibbett, H. D., 1974, "Special Structural Elements for Piping Analysis," in *ASME Special Publication, Pressure Vessels and Piping: Analysis and Computers*, S. Tuba, R. A. Selby, and W. B. Wright, eds., ASME, New York, pp. 1–10.
- [16] Bathe, K. J., and Almeida, C. A., 1982, "A Simple and Effective Pipe Elbow Element-Linear Analysis," *ASME J. Appl. Mech.*, **47**, pp. 93–100.

- [17] Mackenzie, D., and Boyle, J. T., 1992, "A Simple Pipe Bend Element for Piping Flexibility Analysis," *Int. J. Pressure Vessels Piping*, **51**(1), pp. 85–106.
- [18] De Melo, F. J. M. Q., and De Castro, P. M. S. T., 1992, "A Reduced Integration Mindlin Beam Element for Linear Elastic Stress Analysis of Curved Pipes Under Generalized In-Plane Loading," *Comput. Struct.*, **43**(4), pp. 787–794.
- [19] Yin, J. H., Paulin, M. J., Clark, J. I., and Poorooshab, F., 1993, "Preliminary Finite Element Analysis of Lateral Pipeline/Soil Interaction and Comparison to Centrifuge Model Test Results," *Proc. 12<sup>th</sup> International Conference on Offshore Mechanics and Arctic Engineering*, Part 5 (of 6), ASME, New York, pp. 143–155.
- [20] Altaee, A., and Boivin, R., 1995, "Laterally Displaced Pipelines: Finite Element Analysis," *Proc. 14<sup>th</sup> International Conference on Offshore Mechanics and Arctic Engineering*, Part 5 (of 6), ASME, New York, pp. 209–216.
- [21] Altaee, A., Fellenius, B. H., and Salem, H., 1996, "Finite Element Modeling of Lateral Pipeline-Soil Interaction," *Proc. 15<sup>th</sup> International Conference on Offshore Mechanics and Arctic Engineering*, Part 5 (of 6), ASME, New York, pp. 333–341.
- [22] Winkler, E., 1867, *Die leher von der elasticitaet and festigkeit*, Prag, Dominicaus (Czechoslovakia), p. 182.
- [23] Hetenyi, M., 1964, *Beams on Elastic Foundation*, University of Michigan Press, Ann Arbor.
- [24] Vesić, A. S., 1971, "Breakout Resistance of Objects Embedded in Ocean Bottom," *J. Soil Mech. Found. Div.*, **94**(SM9), pp. 1183–1205.
- [25] Audibert, J. M. E., and Nyman, K. J., 1977, "Soil Restraint Against Horizontal Motion of Pipe," *J. Geotech. Eng.*, **103**(GT10), Oct., pp. 1119–1142.
- [26] Peng, L. C., 1978, "Stress Analysis Method for Underground Pipe Lines, Part 1 and 2," *Pipeline Industry*, April and May, Houston, TX.

- [27] Nyman, K. J., 1984, "Soil Response Against Oblique Motion of Pipes," *J. Transp. Eng.*, **110**(2), pp. 190–202.
- [28] Hsu, T. W., 1996, "Soil Restraint Against Oblique Motion of Pipelines in Sand," *Can. Geotech. J.*, **33**(1), pp. 180–188.
- [29] Goodling, E. C., Jr., 1997, "Quantification of Nonlinear Restraint on the Analysis of Restrained Underground Piping," *Proc. 1997 ASME Pressure Vessels and Piping Conference, Pressure Vessels and Piping Division, ASME, New York, PVP*, **356**, pp. 107–116.
- [30] Ng, P. C. F., Pyrah, I. C., and Anderson, W. F., 1997, "Prediction of Soil Restraint to a Buried Pipeline Using Interface Elements," *Numerical Models in Geomechanics Proceedings of the Sixth International Symposium, NUMOG VI*, pp. 469–487.
- [31] Trautmann, C. H., O'Rourke, T. D., and Kulhawy, F. H., 1985, "Uplift Force-Displacement Response of Buried Pipe," *J. Geotech. Eng.*, **111**(9), Sept., pp. 1061–1075.
- [32] Trautmann, C. H., and O'Rourke, T. D., 1985, "Lateral Force-Displacement Response of Buried Pipe," *J. Geotech. Eng.*, **111**(9), Sept., pp. 1077–1092.
- [33] Ovesen, N. K., 1964, "Anchor Slab, Calculation Methods and Model Tests," *Bulletin 16, Danish Geotechnical Institute, Copenhagen, Denmark*.
- [34] Row, R. K., and Davis, E. H., 1982, "The Behavior of Anchor Plates in Sand," *Geotechnique*, **32**(1), March, pp. 25–41.
- [35] Hsu, T. W., 1993, "Rate Effect on Lateral Soil Restraint of Pipelines," *Soils Found.*, **33**(4), pp. 159–169.
- [36] Dickin, E. A., 1994, "Uplift Resistance of Buried Pipelines in Sand," *Soils Found.*, **34**(2), June, pp. 41–48.

- [37] Poorooshasb, F., Paulin, M. J., Rizkalla, M., and Clark, J. I., 1994, “Centrifuge Modeling of Laterally Loaded Pipelines,” *Transport Research Record 1431*, TRB, National Research Council, Washington, D.C., pp. 33–40.
- [38] SMAP-3D, 1999, *SMAP-3D, Structure Medium Analysis Program*, User’s Manual, Version 4.0, Comtech Research, Clifton, Virginia, VA.
- [39] FEMAP, 1996, *FEMAP User’s Manual*, Version 4.5 for Windows, Enterprise Software Products, Inc.
- [40] FEMAP, 1996, *Introduction to FEA Using FEMAP*, Enterprise Software Products, Inc.
- [41] Marston, A., and Anderson, A. O., 1913, “The Theory of Loads on Pipes in Ditches and Tests on Cement and Clay Drain Tile and Sewer Pipe,” *Bulletin 31*, Engineering Experiment Station, Iowa State College, Ames, IA.
- [42] Abduljauwad, S. N., Al-Ghamedy, H. N., Al-Shayea, N. A., and Asi, I. M., 1999, “Behavior, Analysis and Design of Buried Pipelines,” *First Progress Report*, PN 20014, prepared for Saudi Aramco, Dhahran, April.
- [43] ASME B31.1, 1992, “Appendix VII—Nonmandatory Procedures for the Design of Restrained Underground Piping,” *Power Piping*, ASME, New York.
- [44] CGL (Committee on Gas and Liquid Fuel Lines), 1984, *Guidelines for the Seismic Design of Oil and Gas Pipelines Systems*, American Society of Civil Engineers, New York, New York.
- [45] Abduljauwad, S. N., Al-Ghamedy, H. N., Al-Shayea, N. A., and Asi, I. M., 1999, “Behavior, Analysis and Design of Buried Pipelines,” *Second Progress Report*, PN 20014, prepared for Saudi Aramco, Dhahran, October.

- [46] CANDE, 1989, *CANDE-89 Culvert Analysis and Design Computer Program User's Manual*, Report No. FHWA-RD-89-169, Author: S. C. Musser, Federal Highway Administration, VA.
- [47] Siddiqui, J. A., 2000, "The Interaction Between Soil and Buried Bent Pipelines," M.S. thesis, King Fahd University of Petroleum & Minerals, Dhahran, Saudi Arabia.
- [48] Abduljawwad, S. N., Al-Ghamedy, H. N., Al-Shayea, N. A., Asi, I. M., Siddiqui, J. A., and Bashir, R., 2001, "Behavior, Analysis and Design of Buried Pipelines," Final Report, PN 20014, prepared for Saudi Aramco, Dhahran, November.
- [49] Timoshenko, S. P., and Gere, J. M., 1963, *Theory of Elastic Stability*, 2nd ed., McGraw-Hill, New York, U.S.A.
- [50] Antaki, G., 1998, "A Review of Methods for the Analysis of Buried Pressure Piping," Welding Research Council, U.S.A.
- [51] Ellinas, C. P., 1984, *Buckling of Offshore Structures, A State-of-the-Art Review of Buckling of Offshore Structures*, Granada Publishing Ltd., London, U.K.
- [52] Watashi, K., and Iwata, K., 1995, "Thermal Buckling and Progressive Ovalization of Pipes: Experiences at the TTS Sodium Test Facility and Their Analysis," Nucl. Eng. Des., **153**, pp. 319–330.
- [53] Farshad, M., 1994, *Stability of Structure*, Elsevier.
- [54] AWWA C150, 1996, "American National Standard for Thickness Design of Ductile-Iron Pipe," American Water Works Association, Denver, Colorado, U.S.A.
- [55] Moore, I. D., and Booker, J. R., 1985, "Simplified Theory for the Behaviour of Buried Flexible Cylinders Under the Influence of Uniform Hoop Compression," Int. J. Solids Struct., **21**(9), pp. 929–941.

- [56] Moore, I. D., and Booker, J. R., 1985, "Behaviour of Buried Flexible Cylinders Under the Influence of Nonuniform Hoop Compression," *Int. J. Solids Struct.*, **21**(9), pp. 943–956.
- [57] Murray, D. W., 1997, "Local Buckling, Strain Localization, Wrinkling and Postbuckling Response of Line Pipe," *Eng. Struct.*, **19**(5), pp. 360–371.
- [58] Chiou, Y.-J., and Chi, S.-Y., 1996, "A Study on Buckling of Offshore Pipelines," *ASME J. Offshore Mech. Arct. Eng.*, **118**, February, pp. 62–70.
- [59] Hobbs, R. E., 1981, "Pipeline Buckling Caused by Axial Loads," *J. Constr. Steel Res.*, **1**(2), January, pp. 2–10.
- [60] Hobbs, R. E., 1984, "In-Service Buckling of Heated Pipelines," *J. Transp. Eng.*, **110**(2), March, pp. 175–189.
- [61] Taylor, N., and Gan, A. B., 1984, "Regarding the Buckling of Pipelines Subject to Axial Loading," *J. Constr. Steel Res.*, **4**, pp. 45–50.
- [62] Taylor, N., and Gan, A. B., 1986, "Refined Modelling for the Lateral Buckling of Submarine Pipelines," *J. Constr. Steel Res.*, **6**, pp. 143–162.
- [63] Taylor, N., and Gan, A. B., 1987, "Refined Modelling for the Vertical Buckling of Submarine Pipelines," *J. Constr. Steel Res.*, **7**, pp. 55–74.
- [64] Reddy, B., 1979, "An Experimental Study of the Plastic Buckling of Circular Cylinders in Pure Bending," *Int. J. Solids Struct.*, **15**, pp. 669–683.
- [65] Stephens, D. R., 1991, "Pipeline Monitoring—Limit State Criteria," Battle Report NG-18 No. 188 for the American Gas Association, U.S.A.
- [66] Yun, H., and Kyriakides, S., 1985, "Model for Beam-Mode Buckling of Buried Pipelines," *J. Eng. Mech.*, **111**(2), February, pp. 235–253.
- [67] Yun, H., and Kyriakides, S., 1990, "On the Beam and Shell Modes of Buckling of Buried Pipelines," *Int. J. Soil Dyn. Earthquake Eng.*, **9**(4), pp. 179–193.

- [68] Deutsch, W. L., Jr., and R. F. Weston, Inc., 1996, "Determination of the Required Thickness of Soil Cover Above Buried Landfill Gas Transfer Pipes to Prevent Thermal Buckling: An Engineered Approach," Proc. 12<sup>th</sup> (1996) International Conference on Solid Waste Technology and Management, Philadelphia, PA.
- [69] Shaw, P. K., and Bomba, J. G., 1994, "Finite-Element Analysis of Pipeline Upheaval Buckling," Pipeline Technology, ASME, **V**, pp. 291–296.
- [70] Chiou, Y.-J., and Chi, S.-Y., 1993, "Beam Mode Buckling of Buried Pipelines in a Layered Medium," Proc. Third (1993) International Offshore and Polar Engineering Conference, Singapore, 6–11 June, pp. 10–17.
- [71] Zhou, Z., and Murray, D. W., 1995, "Analysis of Postbuckling Behavior of Line Pipe Subjected to Combined Loads," Int. J. Solids Struct., **32**(20), pp. 3015–3036.
- [72] API Recommended Practice 1102, 1993, "Steel Pipelines Crossing Railroads and Highways," American Petroleum Institute, Washington, D.C.
- [73] Jullien, J. F., 1991, *Buckling of Shell Structures on Land, in the Sea and in the Air*, Elsevier.
- [74] Abduljawwad, S. N., Al-Ghamedy, H. N., Al-Shayea, N. A., and Asi, I. M., 2001, "Behavior, Analysis and Design of Buried Pipelines," Fifth Progress Report, PN 20014, prepared for Saudi Aramco, Dhahran, April.
- [75] Abduljawwad, S. N., Al-Ghamedy, H. N., Al-Shayea, N. A., Asi, I. M., Siddiqui, J. A., and Bashir, R., 2001, *Analysis and Design of Buried Pipelines, User's Manual, ADBP Program*, prepared for Saudi Aramco, Dhahran, November.

**List of Tables**

**Table 1** Range of parameters considered in the study

**Table 2** Maximum temperature change

**Table 3** Generated models for the ultimate change in temperature for pipes with horizontal bends

## List of Figures

- Fig. 1** Meshes used to examine the effect of the mesh density for horizontal bends
- Fig. 2** Effect of mesh density on the results of the horizontal movement of buried pipes
- Fig. 3** Comparison of current study with lab test results for lateral movement of pipes
- Fig. 4** Typical buried horizontal pipe bend
- Fig. 5** Soil reaction against movement of buried horizontal bend
- Fig. 6** Location of mesh boundaries
- Fig. 7** Two-dimensional mesh made to extrude a 3D horizontal bend mesh
- Fig. 8** Buried pipe horizontal bend mesh

**Table 1.** Range of Parameters Considered in the Study

Factor	Minimum	Maximum	Comments
Pipe outer diameter, $D$	305 mm (12 in.)	1524 mm (60 in.)	This range is common in the oil industry
Height of overburden from surface to pipe crown, $H_c$	As required	As required	This is usually the needed variable
Pipe bend radius, $R_b$	15 m (50 ft)	213 m (700 ft)	This range is common in the oil industry
Pipe bend angle, $\theta$	1°	90°	This range is common in the oil industry
Diameter/thickness ratio, $D/t$	50	150	This range is common in the oil industry
Internal pressure, $p$	0	*	* The maximum the pipe can carry before reaching the maximum allowable stress
Specific gravity of pipe content, $G_f$	0	1	0 (Gas), 0.56 (LPG), 0.86 (Crude Oil), 1 (Water)
Temperature change, $\Delta T$	0	66.7°C (120°F)	This range is common in the oil industry
Pipe allowable stress	*	*	* Any grade of steel with an appropriate safety factor
Safety factor	*	*	* As specified by the used code/standard ... etc.
Modulus of soil reaction, $E'$	*	*	* Appropriate value for the local soil (for buckling check)
Winkler spring coefficient, $k_o$	*	*	* Appropriate value for the local soil (for buckling check)

**Table 2.** Maximum Temperature Change

S. No.	D mm (in)	H <sub>c</sub> mm (in)	R <sub>b</sub> m (ft)	q (Deg)	D/t	p kPa (psi)	G <sub>f</sub>	Ultimate Maximum Temperature Change °C (°F)
1	300 (12)	200 (8)	15 (50)	15	50	1034 (150)	0	15.81 (28.45)
2	600 (24)	600 (24)	15 (50)	15	50	1034 (150)	0	40.98 (73.77)
3	1050 (42)	300 (12)	15 (50)	15	50	1034 (150)	0	24.96 (44.92)
4	1500 (60)	650 (26)	15 (50)	15	50	1034 (150)	0	48.94 (88.09)
5	300 (12)	150 (6)	90 (300)	15	50	1034 (150)	0	35.91 (64.63)
6	600 (24)	300 (12)	90 (300)	15	50	1034 (150)	0	41.53 (74.75)
7	1050 (42)	200 (8)	90 (300)	15	50	1034 (150)	0	26.58 (47.85)
8	1500 (60)	600 (24)	90 (300)	15	50	1034 (150)	0	53.06 (95.51)
9	1050 (42)	250 (10)	207 (690)	15	50	1034 (150)	0	56.31 (101.36)
10	1500 (60)	300 (12)	207 (690)	15	50	1034 (150)	0	53.27 (95.88)
11	300 (12)	450 (18)	15 (50)	45	50	1034 (150)	0	25.08 (45.14)
12	300 (12)	750 (30)	15 (50)	45	50	1034 (150)	0	47.13 (84.83)
13	600 (24)	1200 (48)	15 (50)	45	50	1034 (150)	0	51.85 (93.33)
14	1050 (42)	1200 (48)	15 (50)	45	50	1034 (150)	0	43.32 (77.98)
15	300 (12)	250 (10)	90 (300)	45	50	1034 (150)	0	63.01 (113.42)
16	600 (24)	375 (15)	90 (300)	45	50	1034 (150)	0	54.85 (98.73)
17	1050 (42)	500 (20)	90 (300)	45	50	1034 (150)	0	47.36 (85.25)
18	1500 (60)	750 (30)	90 (300)	45	50	1034 (150)	0	50.84 (91.52)
19	600 (24)	125 (5)	207 (690)	45	50	1034 (150)	0	60.72 (109.3)
20	1050 (42)	200 (8)	207 (690)	45	50	1034 (150)	0	59.43 (106.97)
21	1500 (60)	250 (10)	207 (690)	45	50	1034 (150)	0	57.32 (103.17)
22	600 (24)	450 (18)	15 (50)	85	50	1034 (150)	0	19.81 (35.65)
23	1050 (42)	600 (24)	15 (50)	85	50	1034 (150)	0	21.68 (39.03)
24	1500 (60)	900 (36)	15 (50)	85	50	1034 (150)	0	30.66 (55.19)
25	300 (12)	250 (10)	90 (300)	85	50	1034 (150)	0	60.73 (109.31)
26	600 (24)	250 (10)	90 (300)	85	50	1034 (150)	0	42.82 (77.07)
27	1050 (42)	300 (12)	90 (300)	85	50	1034 (150)	0	37.03 (66.65)
28	1500 (60)	600 (24)	90 (300)	85	50	1034 (150)	0	52.02 (93.64)
29	600 (24)	125 (5)	207 (690)	85	50	1034 (150)	0	53.81 (96.86)
30	1500 (60)	200 (8)	207 (690)	85	50	1034 (150)	0	56.32 (101.37)
31	1050 (42)	600 (24)	15 (50)	89	50	1034 (150)	0	21.83 (39.3)
32	600 (24)	200 (8)	15 (50)	15	100	1034 (150)	0	17.41 (31.33)
33	1050 (42)	300 (12)	15 (50)	15	100	1034 (150)	0	25.92 (46.65)
34	1500 (60)	450 (18)	15 (50)	15	100	1034 (150)	0	38.28 (68.91)
35	600 (24)	150 (6)	90 (300)	15	100	1034 (150)	0	32.99 (59.38)
36	1050 (42)	200 (8)	90 (300)	15	100	1034 (150)	0	30.76 (55.37)
37	1500 (60)	300 (12)	90 (300)	15	100	1034 (150)	0	38.06 (68.5)
38	1050 (42)	150 (6)	207 (690)	15	100	1034 (150)	0	57.93 (104.28)
39	1500 (60)	250 (10)	207 (690)	15	100	1034 (150)	0	60.87 (109.57)
40	300 (12)	500 (20)	15 (50)	45	100	1034 (150)	0	43.54 (78.37)
41	1050 (42)	900 (36)	15 (50)	45	100	1034 (150)	0	42.91 (77.23)
42	1500 (60)	900 (36)	15 (50)	45	100	1034 (150)	0	41.46 (74.63)

**Table 2.** (Contd.)

S. No.	D mm (in)	H <sub>c</sub> mm (in)	R <sub>b</sub> m (ft)	q (Deg)	D/t	p kPa (psi)	G <sub>f</sub>	Ultimate Max <sup>m</sup> Temperature Change °C (°F)
43	300 (12)	150 (6)	90 (300)	45	100	1034 (150)	0	62.04 (111.68)
44	600 (24)	250 (10)	90 (300)	45	100	1034 (150)	0	61.23 (110.22)
45	1500 (60)	150 (6)	207 (690)	45	100	1034 (150)	0	63.49 (114.28)
46	300 (12)	500 (20)	15 (50)	85	100	1034 (150)	0	51.06 (91.91)
47	600 (24)	600 (24)	15 (50)	85	100	1034 (150)	0	35.28 (63.51)
48	1050 (42)	450 (18)	15 (50)	85	100	1034 (150)	0	20.05 (36.09)
49	600 (24)	250 (10)	90 (300)	85	100	1034 (150)	0	63.42 (114.16)
50	1050 (42)	150 (6)	90 (300)	85	100	1034 (150)	0	33.83 (60.9)
51	1500 (60)	300 (12)	90 (300)	85	100	1034 (150)	0	43.66 (78.58)
52	300 (12)	250 (10)	15 (50)	15	150	1034 (150)	0	28.04 (50.48)
53	1050 (42)	450 (18)	15 (50)	15	150	1034 (150)	0	41.72 (75.1)
54	1500 (60)	150 (6)	15 (50)	15	150	1034 (150)	0	17.51 (31.51)
55	1050 (42)	300 (12)	90 (300)	15	150	1034 (150)	0	49.88 (89.78)
56	1500 (60)	200 (8)	207 (690)	15	150	1034 (150)	0	64.03 (115.25)
57	300 (12)	450 (18)	15 (50)	45	150	1034 (150)	0	49.63 (89.33)
58	1050 (42)	750 (30)	15 (50)	45	150	1034 (150)	0	41.56 (74.81)
59	1500 (60)	750 (30)	15 (50)	45	150	1034 (150)	0	40.38 (72.68)
60	600 (24)	200 (8)	90 (300)	45	150	1034 (150)	0	63.99 (115.19)
61	1500 (60)	350 (14)	90 (300)	45	150	1034 (150)	0	46.88 (84.39)
62	300 (12)	450 (18)	15 (50)	85	150	1034 (150)	0	57.28 (103.1)
63	600 (24)	250 (10)	15 (50)	85	150	1034 (150)	0	16.26 (29.27)
64	1050 (42)	600 (24)	15 (50)	85	150	1034 (150)	0	31.39 (56.51)
65	1500 (60)	750 (30)	15 (50)	85	150	1034 (150)	0	37.56 (67.61)
66	1050 (42)	250 (10)	90 (300)	85	150	1034 (150)	0	54.49 (98.08)
67	1500 (60)	300 (12)	90 (300)	85	150	1034 (150)	0	51 (91.8)
68	600 (24)	300 (12)	15 (50)	15	50	2068 (300)	0	20.38 (36.68)
69	600 (24)	300 (12)	15 (50)	15	150	2068 (300)	0	23.21 (41.77)
70	1500 (60)	600 (24)	15 (50)	45	50	4137 (600)	0	17.4 (31.32)
71	600 (24)	450 (18)	15 (50)	85	100	4137 (600)	0	12.56 (22.6)
72	400 (16)	450 (18)	18 (60)	18	75	689 (100)	0	36.51 (65.71)
73	1000 (40)	450 (18)	18 (60)	18	135	1551 (225)	0	34.86 (62.75)
74	1200 (48)	450 (18)	18 (60)	18	145	1551 (225)	0	37.03 (66.65)
75	600 (24)	300 (12)	15 (50)	15	50	1034 (150)	1	24.45 (44.01)
76	1500 (60)	125 (5)	207 (690)	85	50	1034 (150)	1	60.62 (109.11)
77	600 (24)	300 (12)	15 (50)	15	100	1034 (150)	1	28.89 (52.01)
78	600 (24)	300 (12)	15 (50)	15	100	2068 (300)	1	24.63 (44.33)
79	600 (24)	300 (12)	15 (50)	15	100	4137 (600)	1	16.33 (29.4)
80	600 (24)	300 (12)	15 (50)	15	50	1034 (150)	1	26.86 (48.35)
81	600 (24)	300 (12)	90 (300)	15	50	1034 (150)	1	49.4 (88.92)
82	600 (24)	300 (12)	15 (50)	15	100	1034 (150)	1	32.31 (58.16)
83	1500 (60)	600 (24)	15 (50)	85	150	1034 (150)	1	42.28 (76.1)
84	600 (24)	300 (12)	15 (50)	15	100	4137 (600)	1	19.02 (34.23)

**Table 3.** Generated Models for the Ultimate Change in Temperature for Pipes with Horizontal Bends

Bend angle range (degree)	Generated model	R <sup>2</sup>	Significance level
1 to 15	$\Delta T = \exp(2.6624 + 2.8630 (1/D) + 0.1504 \ln(H_c)^2 + 0.0050 * \ln(R_b)^3 + 0.0215 \ln(D/t)^2 - 0.0049 \ln(p)^3 + 0.2430 \sin(G_f))$ $H_c = \exp(\text{sqr}(-1/0.150444872 * (-\ln(\Delta T) + 2.662435026 + 2.863012799 * (1/D) + 0.00498723 * (\ln(R_b))^3 + 0.021494769 * ((\ln(D/t))^2) - 0.004903904 * ((\ln(p))^3) + 0.243028794 * \sin(G_f))))$	0.8760	0.000
15 to 45	$\Delta T = \exp(1.1504 + 9.8992 (1/D) + 0.1439 \ln(H_c)^2 + 0.0085 * \ln(R_b)^3 + 0.0418 \ln(D/t)^2 - 0.0028 \ln(p)^3 + 0.5875 \sin(G_f))$ $H_c = \exp(\text{sqr}(-1/0.143914931 * (-\ln(\Delta T) + 1.150442228 + 9.899199263 * (1/D) + 0.008489649 * (\ln(R_b))^3 + 0.041841457 * ((\ln(D/t))^2) - 0.002808507 * ((\ln(p))^3) + 0.587458711 * \sin(G_f))))$	0.9141	0.000
45 to 90	$\Delta T = \exp(1.1615 + 10.3646 (1/D) + 0.1452 \ln(H_c)^2 + 0.0090 * \ln(R_b)^3 + 0.0429 \ln(D/t)^2 - 0.0033 \ln(p)^3 + 0.3897 \sin(G_f))$ $H_c = \exp(\text{sqr}(-1/0.14486272 * (-\ln(\Delta T) + 1.145349048 + 10.40450493 * (1/D) + 0.009050572 * (\ln(R_b))^3 + 0.043731911 * ((\log(D/t))^2) - 0.003289856 * ((\ln(p))^3) + 0.384166412 * \sin(G_f))))$	0.9491	0.000

$\Delta T$  = ultimate change in temperature, °F

$R_b$  = radius of bend, ft

$D/t$  = diameter to pipe wall thickness

$t$  = pipe wall thickness, in.

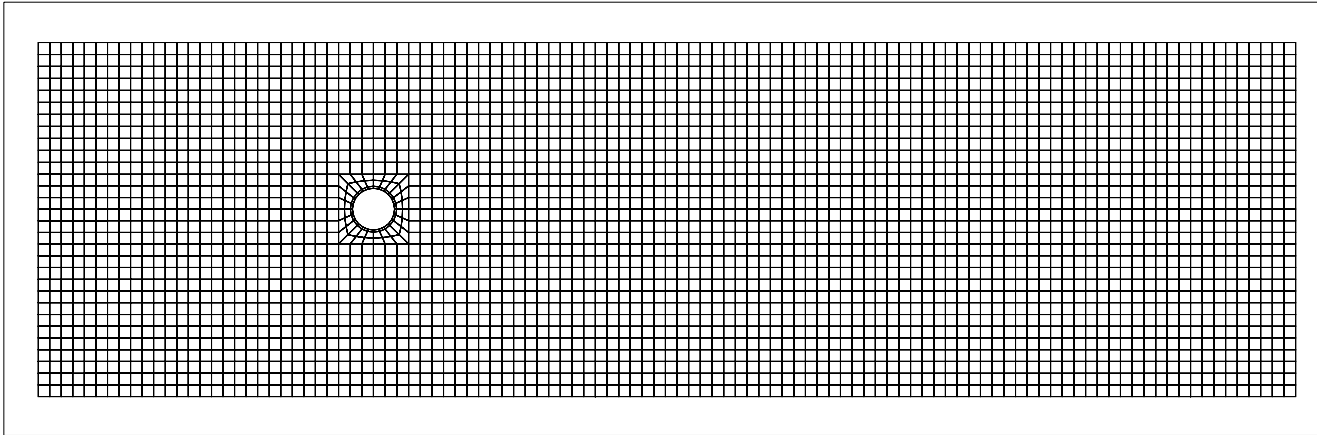
$p$  = internal pressure, psi

$H_c$  = depth of cover, in.

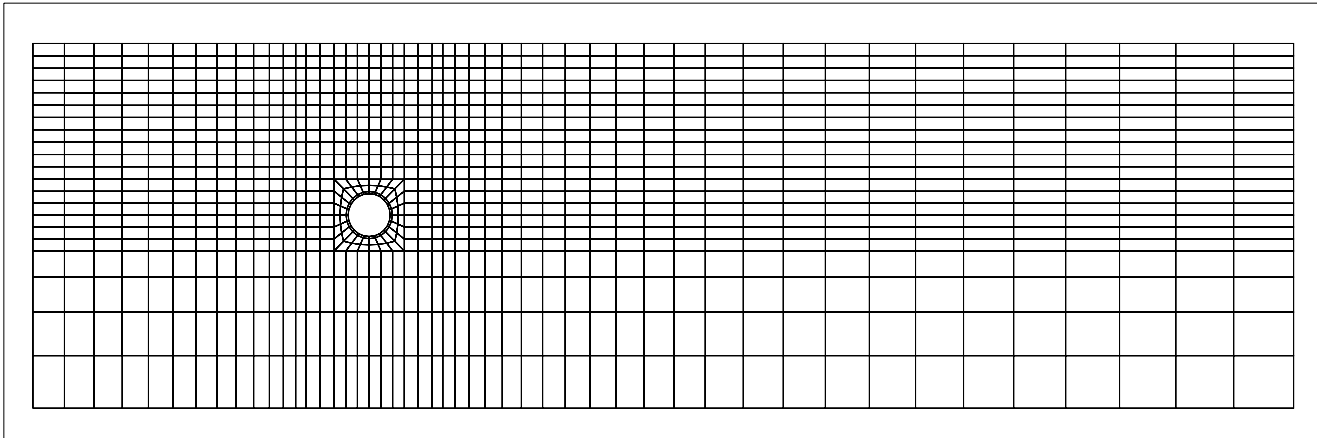
$G_f$  = carried material specific gravity

To convert from °F to °C :  $\Delta T$  (°C) = [ $\Delta T$  (°F)] 5/9

To convert from in. to mm :  $H_c$  (mm) = [ $H_c$  (in.)] 25.4

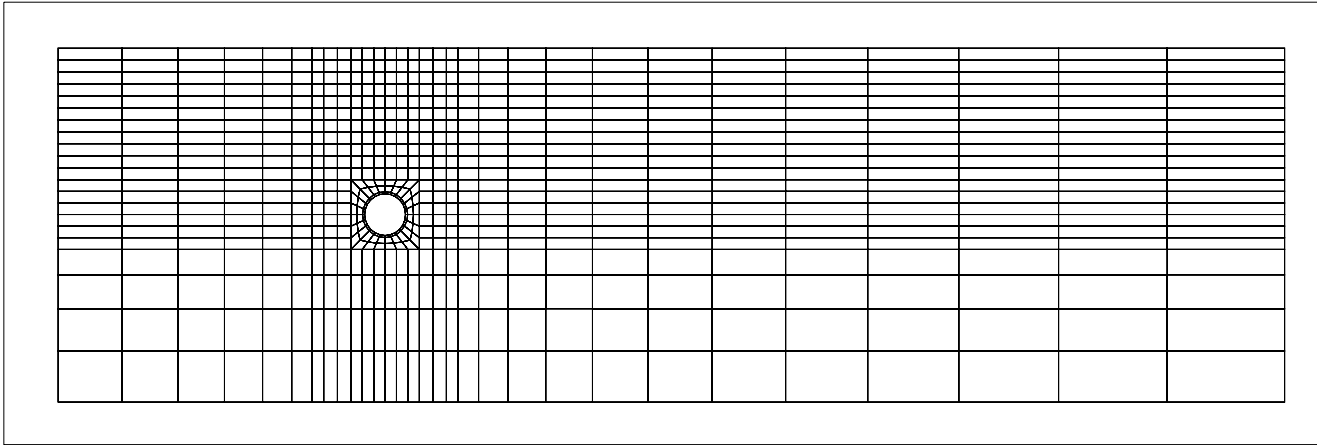


(a) Fine mesh

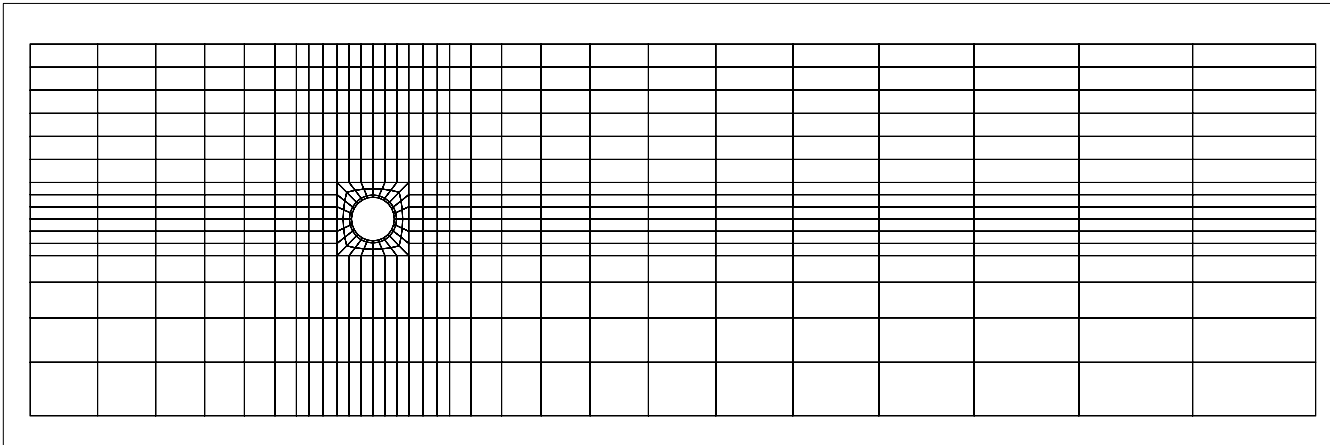


(b) Course mesh 1

Fig. 1 Meshes used to examine the effect of the mesh density for horizontal bends



(c) Course mesh 2



(d) Course mesh 3

Fig. 1 (Contd.)

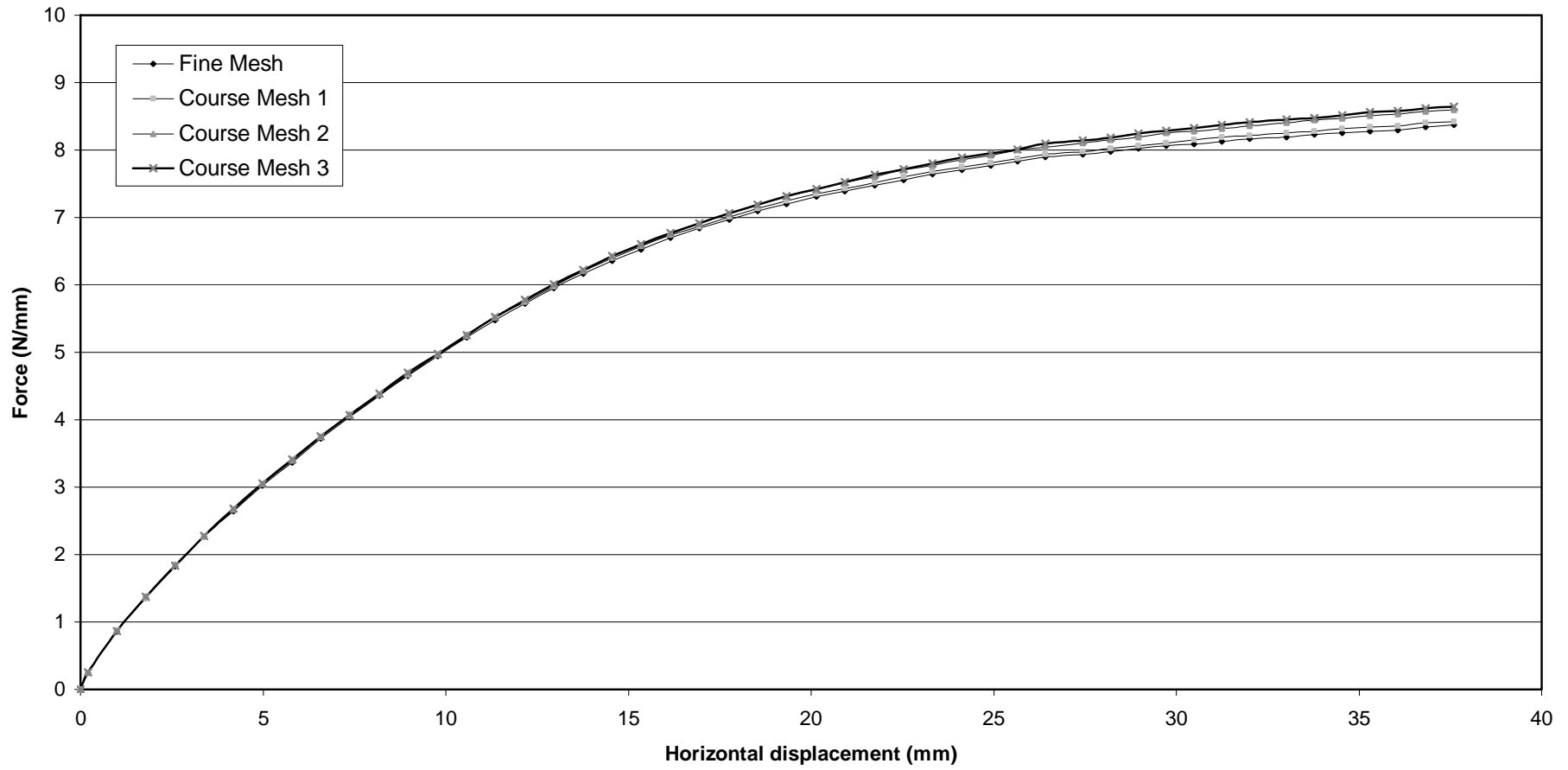


Fig. 2. Effect of mesh density on the results of the horizontal movement of buried pipes

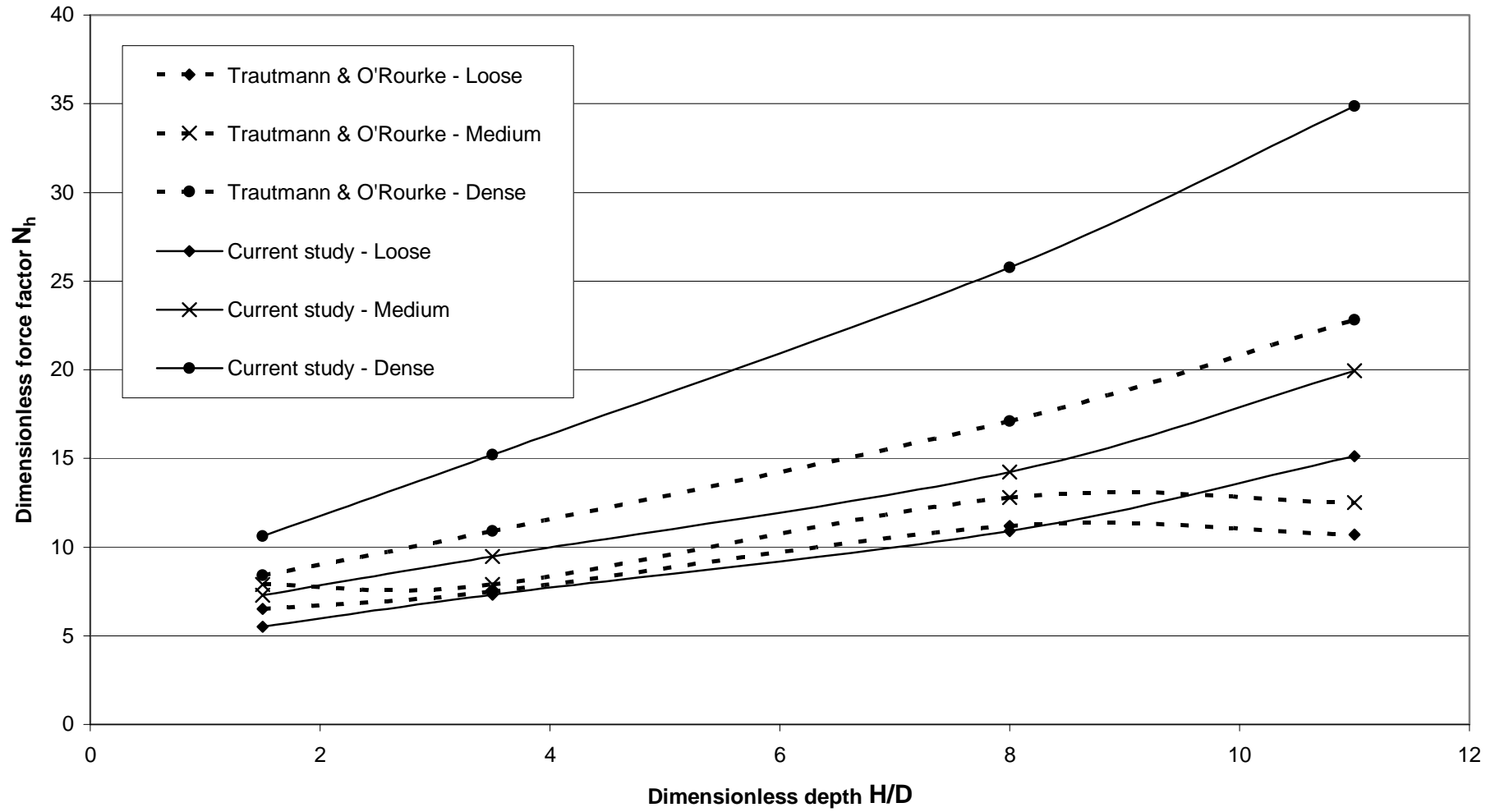
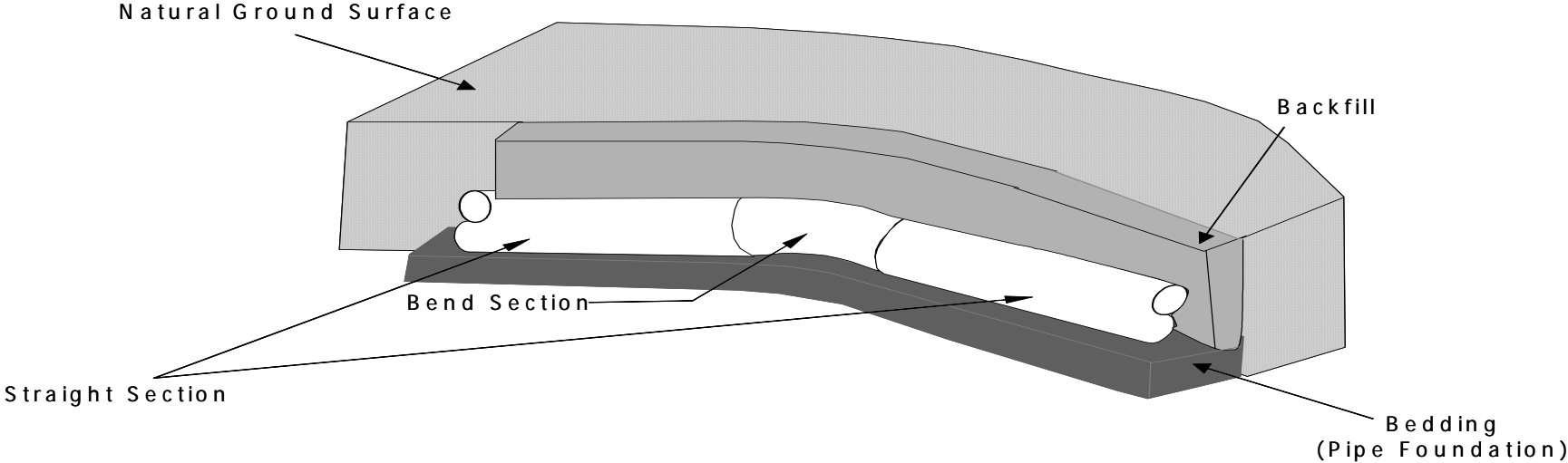
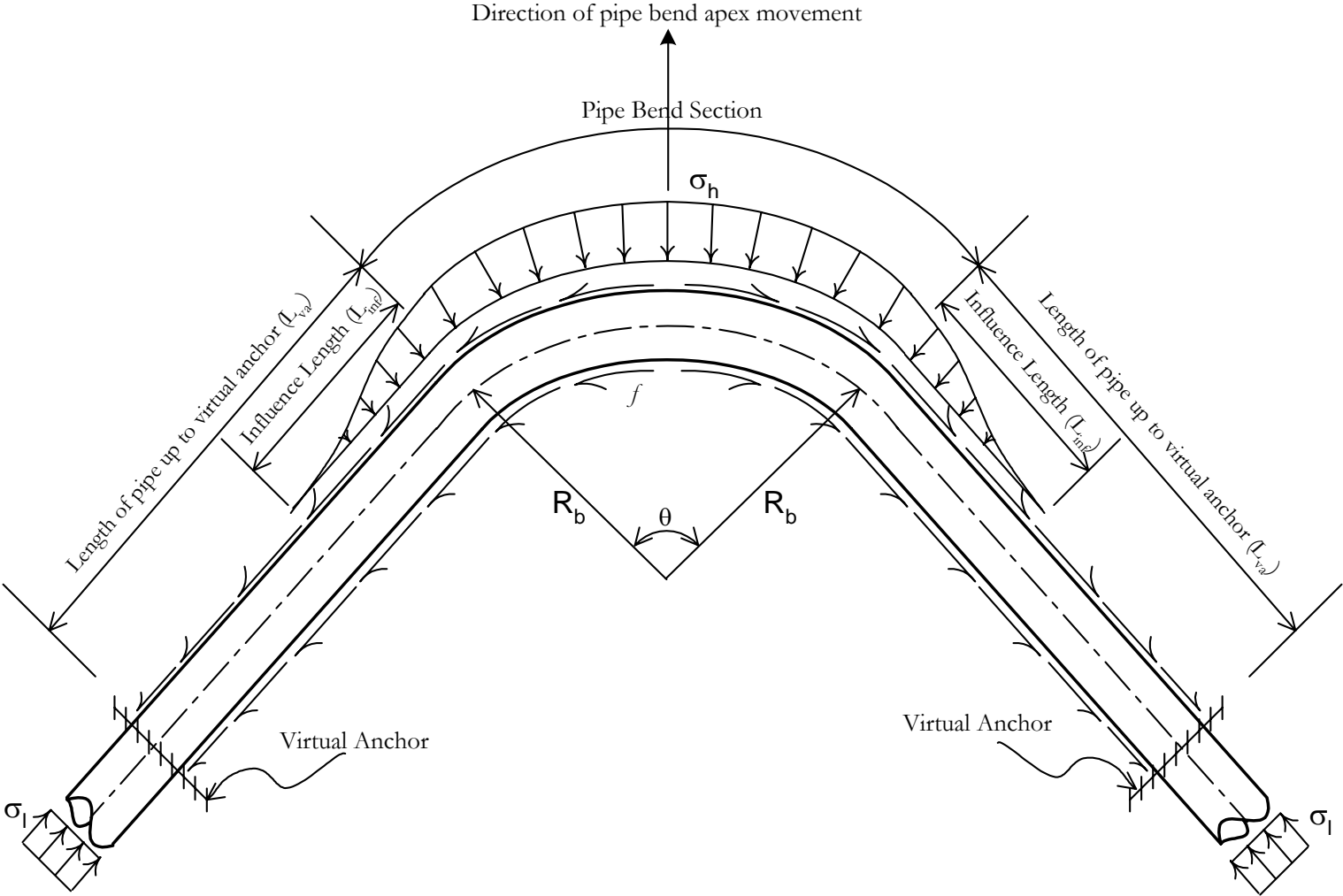


Fig. 3. Comparison of current study with lab test results for lateral movement of pipes



(a) Perspective sectional view

FIG. 4 Typical Buried Horizontal Pipe Bend



(b) Horizontal bend top view showing key parameters

Fig. 4 (Contd.)

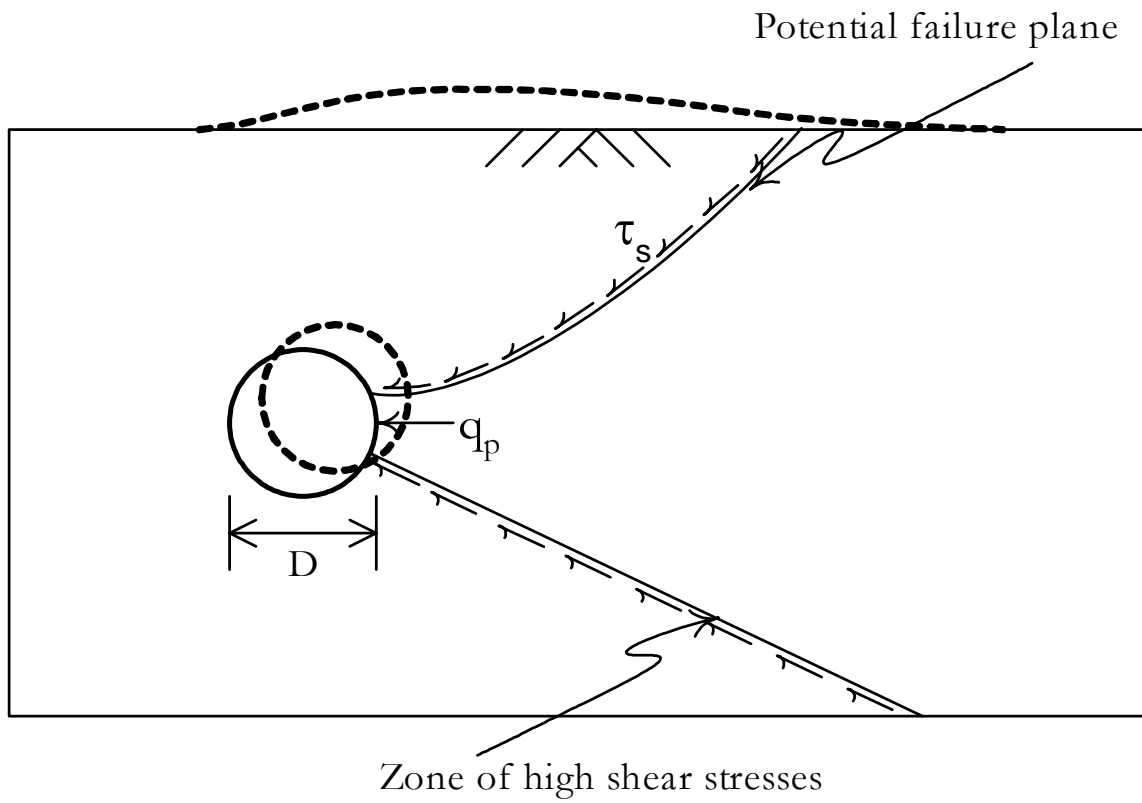
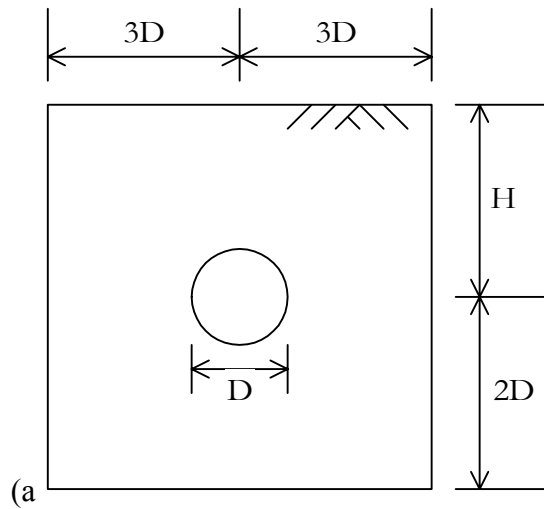
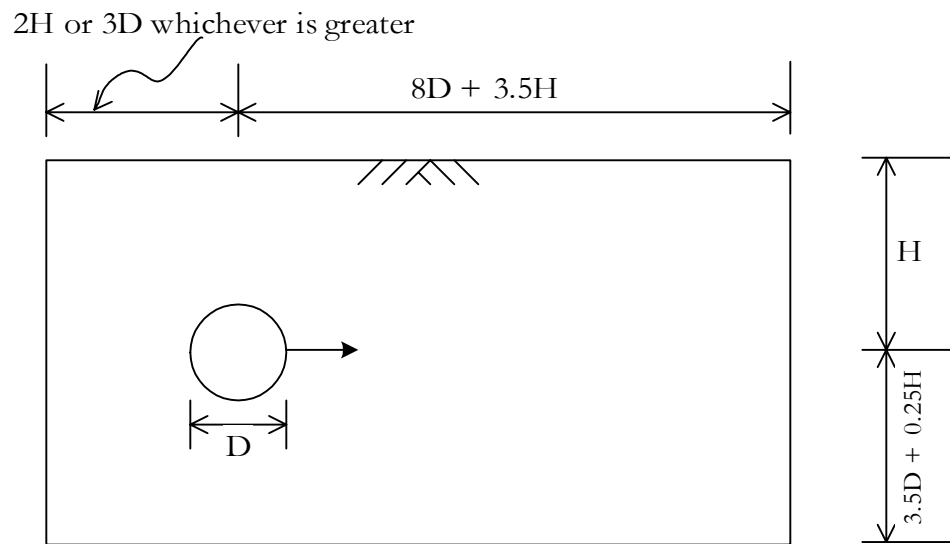


Fig. 5 Soil reaction against movement of buried horizontal bend



(a) Limits for pipe under gravity loading



(b) Limits for pipe moving under lateral forces

Fig. 6 Location of mesh boundaries

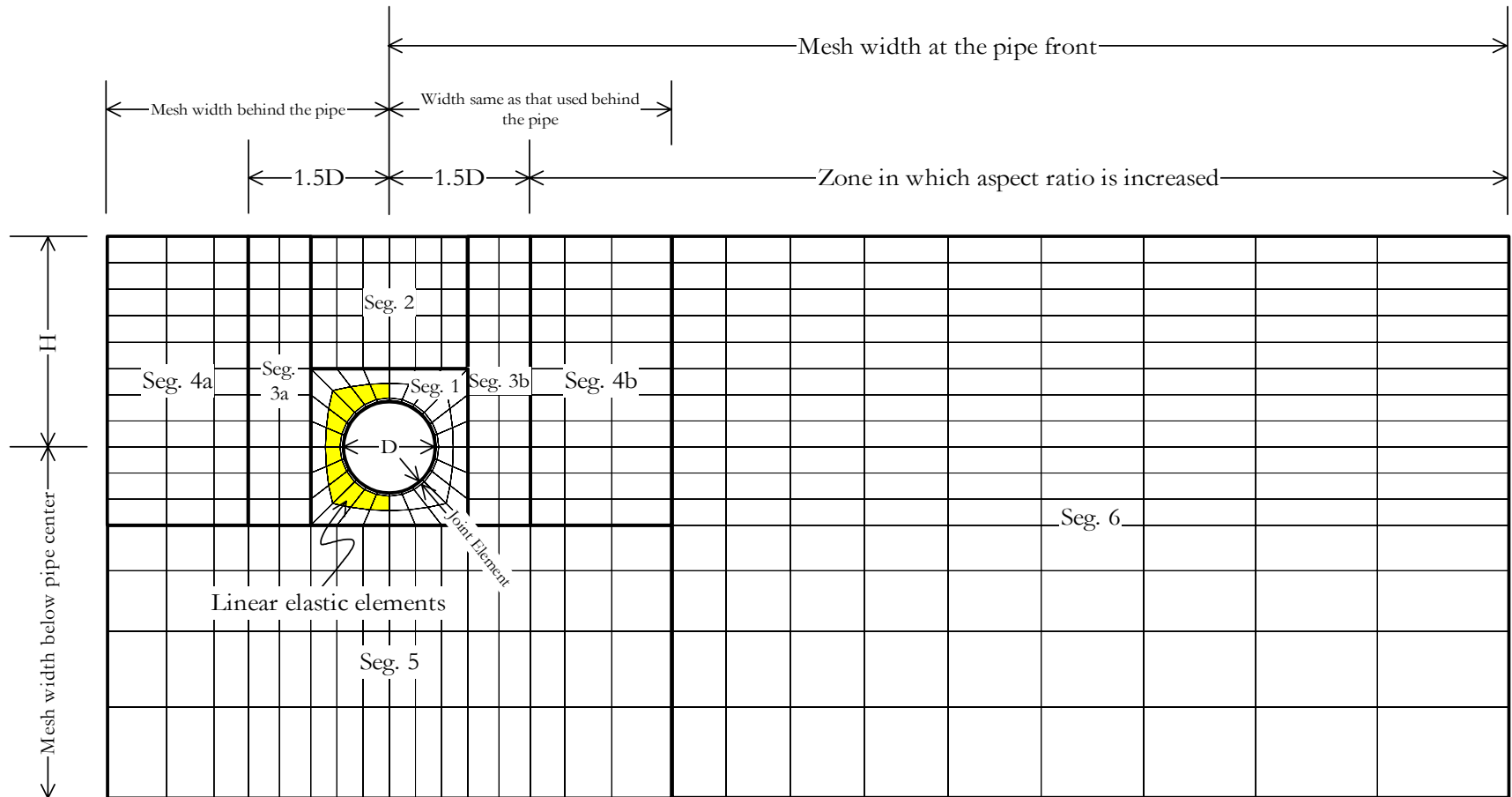
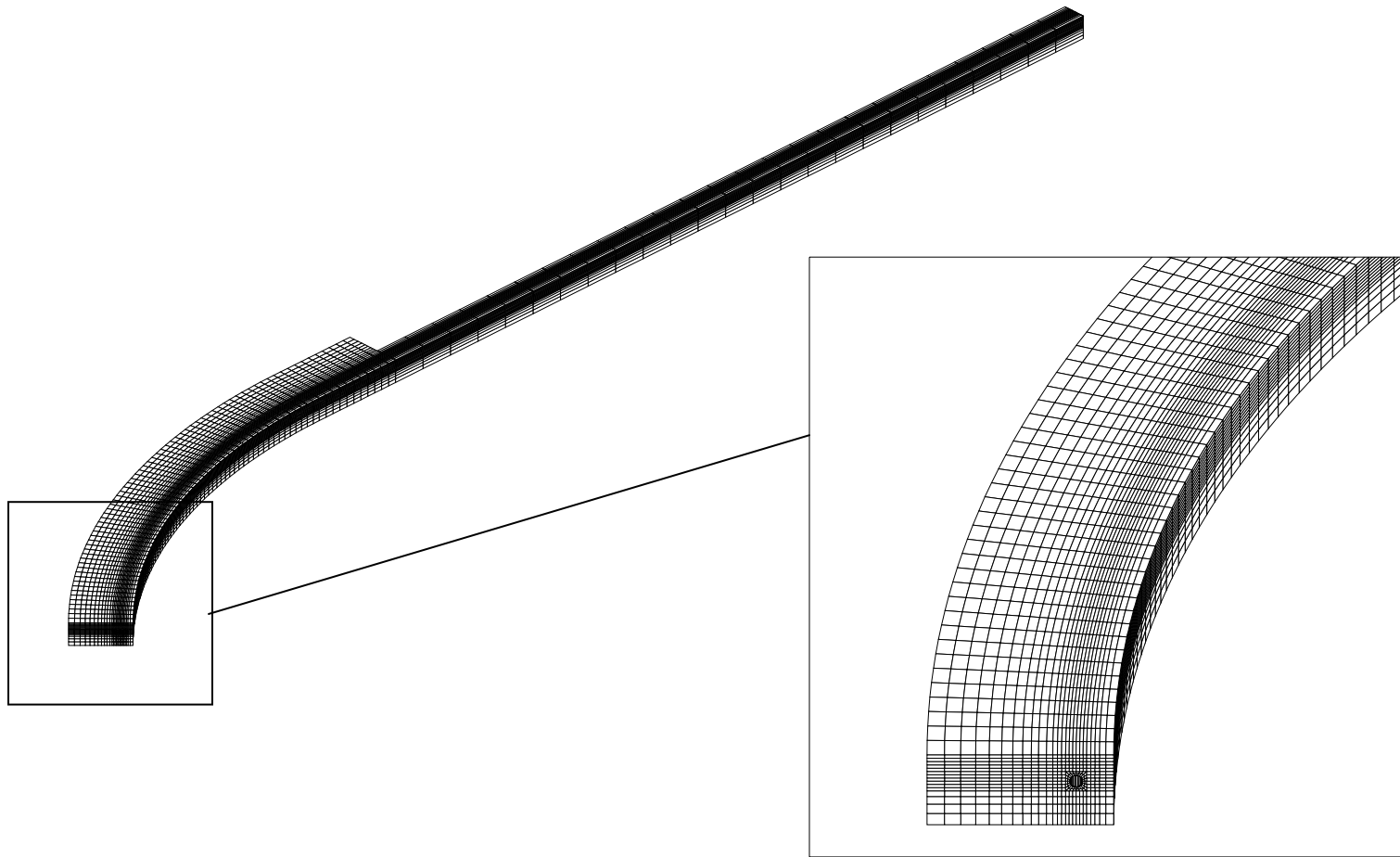
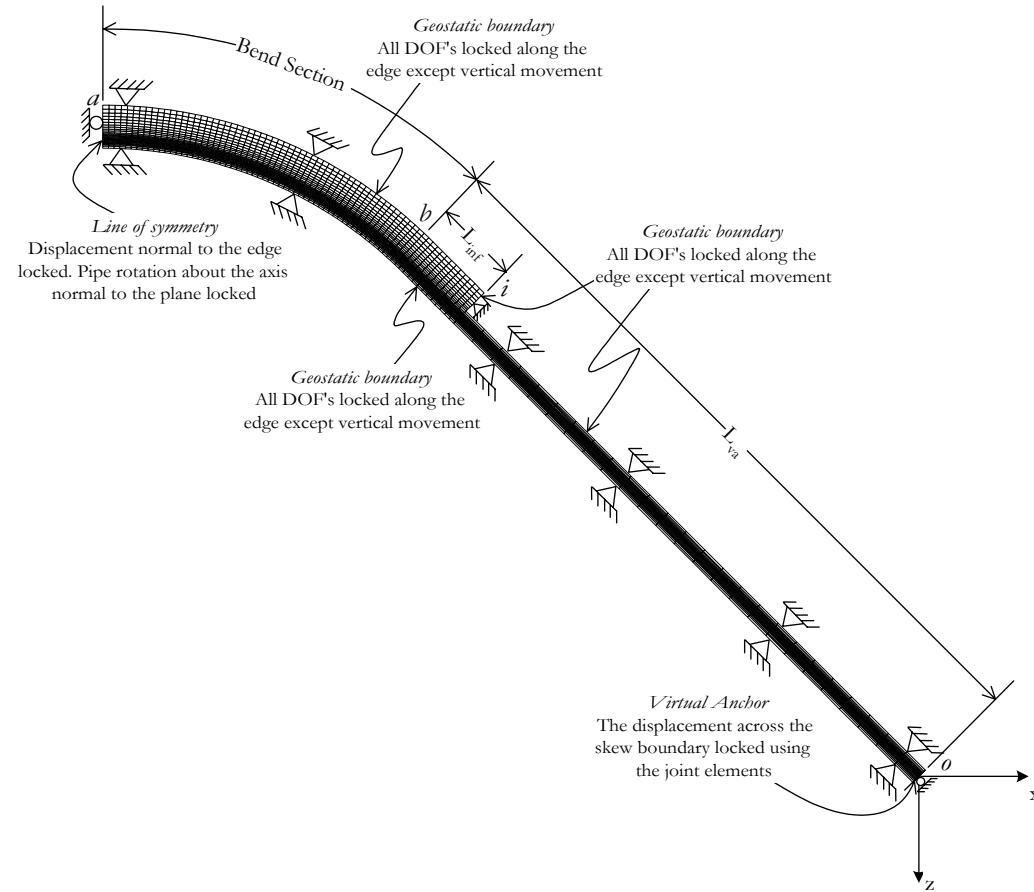


Fig. 7 Two-dimensional mesh made to extrude a 3D horizontal bend mesh



(a) Perspective view

Fig. 8 Buried pipe horizontal bend mesh



(b) Plan

Fig. 8 (Contd.)